FATIGUE CRACK INITIATION AND GROWTH IN TITANIUM ALLOY MATRIX COMPOSITE

T. TAGAWA, E. WADAHARA AND T. MIYATA

Department of Materials Science and Engineering, Nagoya University, Nagoya 464-01, Japan

ABSTRACT

Fatigue crack initiation and growth in titanium alloy composites reinforced with TiC particles and TiB whiskers were investigated. The composites were Ti-6wt%Al-4wt%V reinforced with 10 vol% of TiC particles having an average diameter of 12 μm and Ti-8wt%Al reinforced with 8 vol% of TiB whiskers having an average length of 44 μm and diameter of 4 μm, produced in-situ by the vacuum arc remelting process. Fatigue strength of the composites in notched specimens is less than that of Ti-6wt%Al-4wt%V alloy, while the static strength is higher in both composites. Direct observations in scanning electron microscope by in-situ fatigue tests revealed that fatigue cracks in composites initiated from the cracking of the reinforcing particles or whiskers and the early cracking and its growth to matrix reduced the fatigue lives of the composites. Deterioration in fatigue strength is dominant in the TiC*p*/Ti composite since the fatigue life is governed by the size of initial cracks, that is, the size of reinforcement. On the other hand, fatigue crack growth rate is dependent on the type of the reinforcement. The particulate TiC reinforcement increases the growth rate due to their cracking and debonding at interface, while the TiB whisker decreases the growth rate through the crack deflection and the fiber bridging mechanisms.

KEYWORDS

Metal matrix composite, fatigue, crack initiation, crack growth rate, TiC, TiB

INTRODUCTION

Metal matrix composites (MMC) have many possibilities as advanced materials for various fields. In particle reinforced composites characteristics of the interface between particles and matrix play an important role in deformation and fracture behavior. Many processes for fabricating the particle reinforced MMCs are proposed, but it is difficult to control the chemical reaction at the interface. In a certain case (Manoharan and Lewandowski, 1990), the strength of composite is lower than the matrix alloy due to the deterioration of the interfacial strength. Recently, a MMC fabricating process with the metallurgical precipitating particles is industrially developed. This composite has chemically and mechanically better cohesive interfaces, because the particles themselves are produced by chemical reaction. The reacting systems for this process are restricted in particular composite systems and titanium systems are usually adopted because of high chemical activity. Titanium matrix composites fabricated by this precipitating process are being applied for automobile engine members due to their high strength at high temperature (Saito *et al.*, 1993). However, the practical properties such as fatigue behaviors are not yet clarified for Ti-matrix composites. In this work, the fatigue behaviors for two types of the particles reinforced titanium matrix composites fabricated by the above process were studied. The behaviors of the reinforcing particles at the fatigue crack initiation and the crack growth were investigated.

EXPERIMENTAL PROCEDURE

Materials tested in this work were two types of titanium matrix composites and an alloy Ti-6Al-4V. The composite systems were TiC particles reinforced Ti-6Al-4V alloy and the TiB whiskers reinforced Ti-8Al alloy. The reinforcing particles were precipitated during a vacuum arc remelting of the compacted raw powders. After solidification, the composites were finished with hot rolling and heat treatment. The chemical compositions of materials are listed in Table 1. Hereafter, the materials are designated as TiC*p*/Ti, TiB*w*/Ti and Ti-6Al-4V. Figure 1 shows the

Table 1 Chemical compositions of materials tested. (wt%)

	Al	V	Fe	Cr	C	O	H	Mo	B	Ti
TiC*p*/Ti	6.4	3.7	0.06	10.2	1.1	0.06	0.005	-	-	bal.
TiB*w*/Ti	8.0	0.4	0.07	-	-	0.10	0.019	0.5	11	bal.
Ti-6Al-4V	6.3	4.0	0.19	-	0.01	0.11	0.003	-	-	bal.

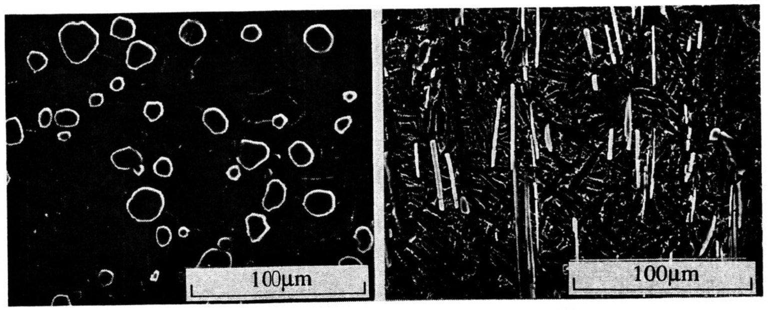

(a) TiC*p*/Ti (b) TiB*w*/Ti

Fig.1 Microstructures of composites tested.

microstructures of the composites observed by a scanning electron microscopy. In the TiC*p*/Ti, spherical TiC particles were dispersed in β-Ti matrix. On the other hand, the TiB particles is of whisker shaping and the matrix is α-Ti. The Ti-6Al-4V showed conventional α and β microstructure. The particle dispersion was almost homogeneous in the TiC*p*/Ti. The TiB*w* particles were aligned with the rolling direction due to their high aspect ratio. The volume fractions and the sizes of the reinforcements in MMCs are listed in Table 2. All specimens were cut to align the loading directions with the rolling direction.

To evaluate the static strengths, tensile tests were performed for smooth cylindrical tensile specimens with a gauge diameter of 6 mm at a rate of 0.001 mm/sec. The strain were measured from an extensometer at a gauge length of 12.7 mm.

Fatigue tests to determine the S-N relations were performed at room temperature with notched round bar specimens as shown in Fig. 2(a). The surface of the notch tip was put off with chemical polishing over 30 µm in depth and finished with buffing. Specimens were uniaxially loaded by a hydraulic servo tester with a frequency of 20 Hz and with a stress ratio $R = \sigma_{min} / \sigma_{max}$, of 0.1. Fracture surfaces were observed by a scanning electron microscopy.

The fatigue crack growth tests were carried out with compact tension specimens at a stress ratio, R = 0.1. The threshold stress intensity factor range ΔK_{th} were determined under the ΔK decreasing control, then, the crack growth rates were measured for the increasing ΔK condition. The ΔK_{th}-s were evaluated at a crack growth rate da/dN of 1 X 10^{-10} m/cycle. During fatigue crack growth, load for crack closure was monitored with the strain gauges adhered on the specimen's

Table 2 Volume fraction and size of particles in composites tested.

		Volume fraction (%)	Average size (mm)	Aspect ratio
TiC*p*/Ti		10.2	12.1 (diameter)	1.6
TiB*w*/Ti	(L-dirention)	8.0	43.7 (length)	10.3
	(T-direction)		15.3	5.8

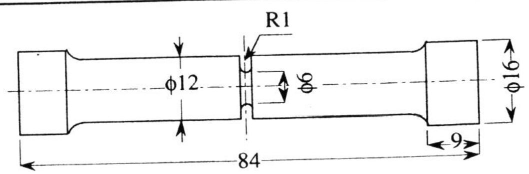

(a) Notched round bar specimen

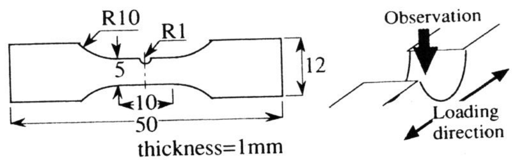

thickness=1mm

(b) Plate specimen for SEM observation

Fig.2 Specimens, units are in mm.

back face. Loading of specimens was stopped prior to the final fractures and the cracked specimens were cut on the mid section in thickness. The fatigue crack paths and the damage particles around the cracks were observed by a scanning electron microscopy after polishing.

For the TiB*w*/Ti and the Ti-6Al-4V, fatigue tests were also performed in a scanning electron microscope for the direct observation. The specimen configuration is shown in Fig. 2(b). The notch surfaces were finished similarly to the notched round bar specimens. Specimens were loaded at a stress ratio of 0.1 and the fatigue crack initiation sites at the notch bottom were observed.

RESULTS AND DISCUSSION

Figure 3 shows the static stress-strain relations for the materials tested. Both the composites showed from 10 to 15 per cent higher strengths than that of the Ti-6Al-4V. In the fatigue life under cyclic loading, however, the relative relation between the materials is far different from the relation in the static strength, as shown in Fig. 4. In spite of a large scatter of the fatigue life in the TiB*w*/Ti, the fatigue lives of the composites were shorter than the Ti-6Al-4V under all stress levels. Figure 5 shows the fractographs observed by SEM for composites. These photos show regions that might be the fatigue crack initiation points at the notch tip. The fracture appearances are different for fatigue stress levels. On the crack initiation sites fractured under relatively high fatigue stresses, cracked particles at the notch tips were observed, shown in Fig. 5(b) and (d). However, in the specimens fractured under low fatigue stresses, the flat surfaces getting the loading direction at an angle of 45 degree were observed, shown in Fig. 5(a) and (c). This dependence of the fracture appearance on the fatigue stress levels was almost the same between TiC*p*/Ti and TiB*w*/Ti. The difference of the fracture appearance at the crack initiation regions shows as the open and solid marks in Fig. 4.

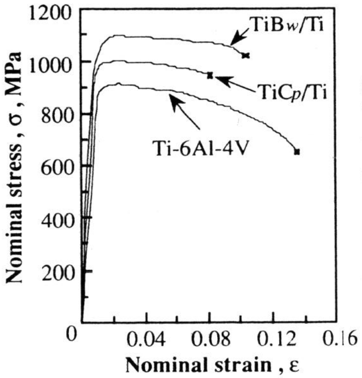

Fig.3 Relations between stress and strain for materials tested .

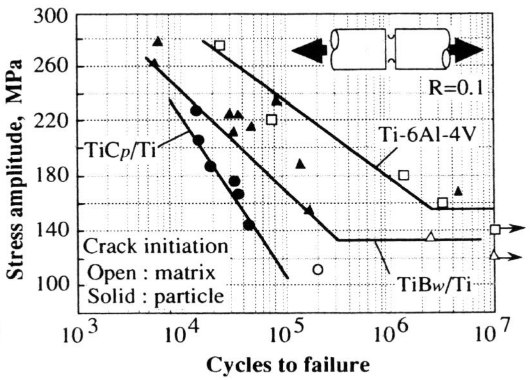

Fig.4 S-N relations of materials tested.

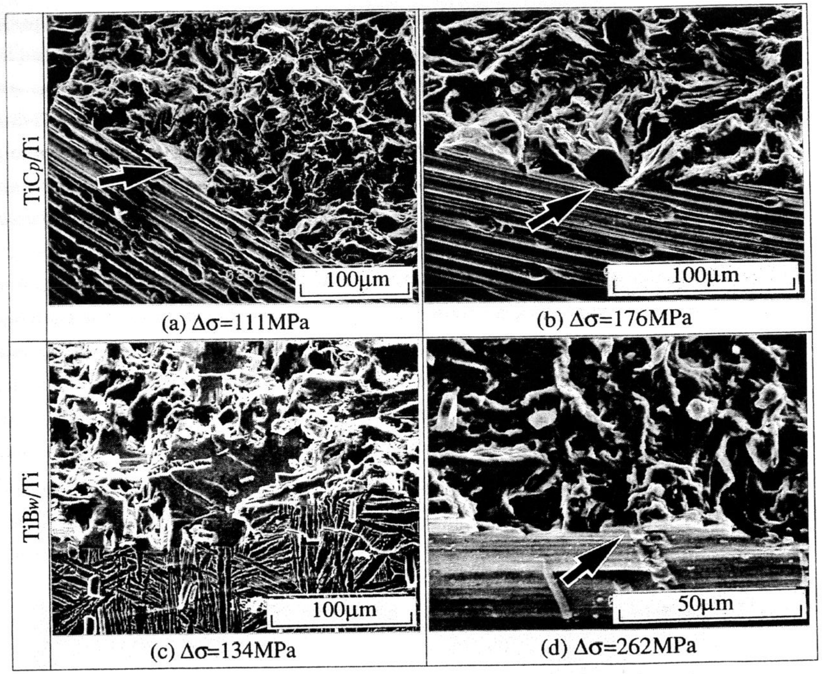

Fig.5 Fractographs of crack initiation point observed in notched round bar .

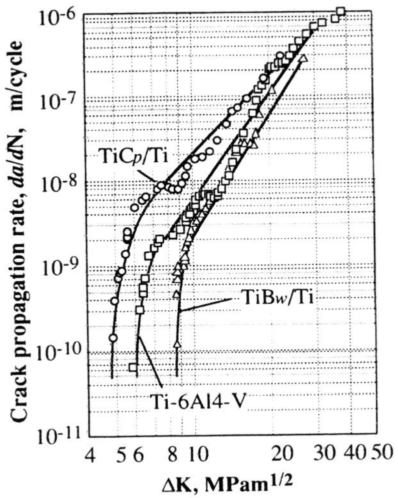

Fig.6 Relation between crack propagation rate and stress intensity factor range.

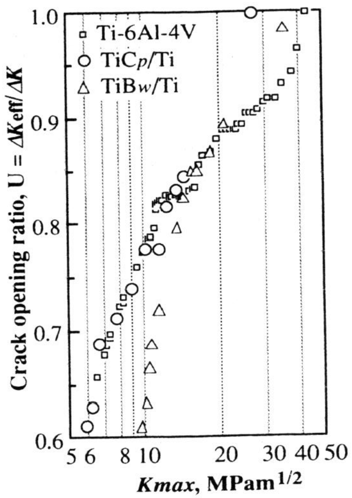

Fig.7 Variations of crack opening ratio with *Kmax* during *ΔK* increasing.

Figure 6 shows the fatigue crack growth rate as a function of the stress intensity factor range, ΔK for all materials. The results indicate that the crack growth rate for TiCp/Ti is the fastest and the rate for TiBw/Ti is the slowest in all ΔK range. In the ΔK_{th}, the TiBw/Ti shows about 45 per cent higher value than the Ti-6Al-4V, and the TiCp/Ti shows about 20 per cent lower than the Ti-6Al-4V. Figure 7 shows the crack opening ratio $\Delta K_{eff}/\Delta K$ obtained during the ΔK increasing condition as a function of the maximum stress intensity factor K_{max}. The TiBw/Ti shows the large crack closure especially in the low stress intensity factor. The TiCp/Ti shows the almost similar crack closing behavior to the Ti-6Al-4V.

Figure 8 shows SEM micrographs of the crack paths for both MMCs observed on the mid sections of the CT specimens. The crack paths are shown both at around the threshold level and at a high level in the stress intensity factor for each composite. In the TiCp/Ti, the crack around a threshold level was propagated straight connecting the interfaces between the particles and the matrix, shown in Fig. 8(a). The stress mismatching at the interface was expected to result in this crack path. The TiC particles do not act as crack resistor and the crack may grow faster due to stress mismatching. On the other hand, the crack under the high stress intensity factor went deflectively to connect the damaged particles around the crack tip, shown in Fig. 8(b). Some of the damaged particles and the secondary cracks were also observed. Although the damaged particles may

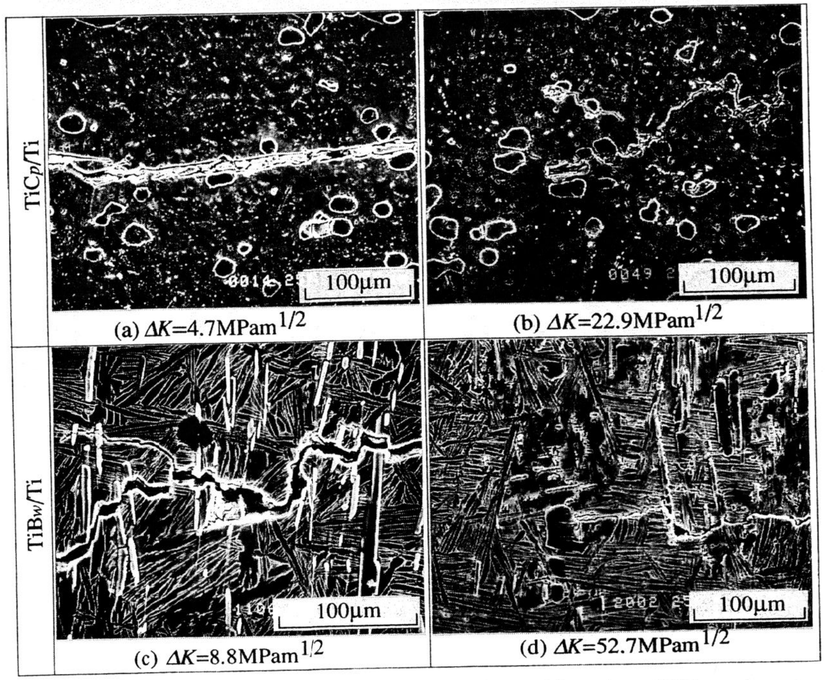

(a) ΔK=4.7MPam$^{1/2}$ (b) ΔK=22.9MPam$^{1/2}$

(c) ΔK=8.8MPam$^{1/2}$ (d) ΔK=52.7MPam$^{1/2}$

Fig.8 SEM micrographs of crack pathes observed on mid section of CT specimens.

provide a crack shielding effect, the particle size is so large that the damaged particles may act as only the defects at the crack tip. In the crack growth of TiBw/Ti, the TiB whisker for the crack near a threshold stress intensity factor shows the many crack bridgings, shown in Fig. 8(c). Although many damaged particles exist around the crack under a high stress intensity factor, similarly to the TiCp/Ti, the crack sizes in TiB whiskers were smaller than in TiC particle because of an acicular shape of the TiB whiskers. The difference of the particle width may be one reason why the crack growth rate in the TiBw/Ti smaller than in the TiCp/Ti.

Figure 9 shows the fatigue crack initiations for Ti-6Al-4V observed in the fatigue tests under the SEM observations. The failure life of this specimen was 4.7 X 10^5 cycles and the fatigue crack initiation was observed at 53 per cent of the total life. On the other hand, Fig. 10(a) shows the crack initiation of the TiBw/Ti under a relatively high stress amplitude. The crack initiated in the TiB whiskers at only the 4 per cent of the failure life; 2.4 X 10^5 cycles. Under the low stress amplitude, crack initiated at the matrix or the interfaces shown in Fig. 10(b). In this case, crack initiations were observed at 11 per cent of the total life. These tendencies agree with the appearances of the fracture initiation regions observed in the round bar fatigue specimens. The mechanisms of the fatigue crack initiation in TiCp/Ti are expected to be similar to the TiBw/Ti.

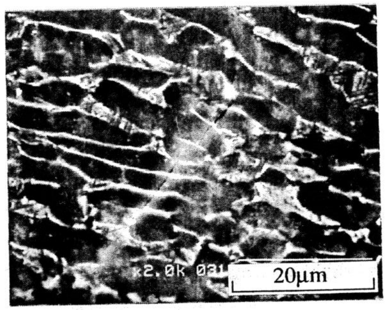

Fig.9 Fatigue crack initiation for Ti-6Al-4V.
(N/Nf=0.53, Nf=4.7X10^5)

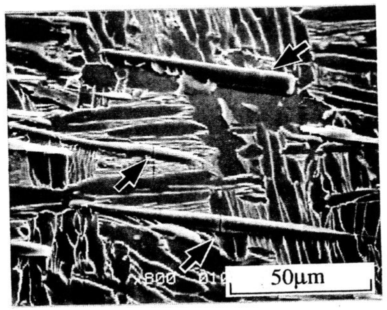

(a) under high stress amplitude. (N/Nf=0.04, Nf=2.4X10^5)

(b) under low stress amplitude. (N/Nf=0.11, Nf=1.0X10^7)

Fig.10 Fatigue crack initiations for TiBw/Ti.

The matrix of the composites is different from Ti-6Al-4V. Therefore, the difference of the fatigue behaviors for the materials tested in this work may not completely be concluded from the effect of the particle composing. The cracking of the reinforcing particles at a first stage of the fatigue damage, however, should make the fatigue life to deteriorate. In the TiC*p*/Ti, the crack size at first stage is large and the crack growth rate is also high because of the large damaged particle size. The short fatigue life of TiC*p*/Ti may result from a short crack initiation life and a high crack growth rate. On the other hand, in the TiB*w*/Ti, the crack growth rate is small due to the an acicular shape of TiB whiskers. Even in the higher crack resistant material TiB*w*/Ti, the fatigue life is not longer than the Ti-6Al-4V. It seems that fatigue life is controlled by the early cracking of the TiB whiskers. The composites tested in this work have better interfacial strength because of the in-situ precipitating process, and the static strength is higher than a base alloy without much loss in elongation. Under fatigue loading, however, the particles cracked at the early stage of the fatigue damage act as initial defect. This may result from a stress mismatch at the interface. The cyclic softening of titanium alloy has been reported (Hatanaka *et al.*, 1991) and the mismatching stress at the interface may increase with the cyclic loading.

CONCLUSIONS

The fatigue crack initiation and growth for the titanium matrix composites fabricated by the in-situ precipitating process were investigated and the conclusions obtained are as follows.

1) The fatigue lives of the composites were smaller than a conventional Ti-6Al-4V alloy, in spite of higher static strengths of the composites.

2) The TiC*p*/Ti composite showed a lower fatigue crack resistance and the TiB*w*/Ti composite showed a higher fatigue crack resistance than Ti-6Al-4V. The difference of the crack growth resistance in the both composites is mainly dependent on the particle shapes and sizes.

3) The deteriorations in the fatigue lives for the both composites resulted from the cracking in the reinforcing particles at the early stage of the fatigue loading.

REFERENCE

Hatanaka, K., T. Fujimitsu and S. Nishida (1991). Elastic-plastic crack growth and life assessment in Ti-6Al-4V alloy under low-cycle fatigue. *Trans. Japan Mech. Eng.*, **57**, 244-249.

Manoharan, M. and J. J. Lewandowski (1990). Crack initiation and growth toughness of an aluminum metal-matrix composite. *Acta Metall.*, **38**, 489-496.

Saito, T., T. Furuta and T. Yamaguchi (1993). A low cost titanium alloy matrix composite. *Proc. 3rd Japan Int. SAMPE sympo.*, 1810-1817.